2022 IEEE/RSJ International Conference on Intelligent Robots and Systems (IROS)
October 23-27, 2022, Kyoto, Japan

Generating Families of Optimally Actuated Gaits from a Legged System's Energetically Conservative Dynamics

Maximilian Raff[1] Nelson Rosa Jr.[1] C. David Remy[1]

***Abstract*— We present a homotopic approach to generating energetically optimal gaits for legged robots that maps passive (i.e., unactuated) gaits of an energetically conservative model of the robot to a model with user-defined target dynamics with dissipation and actuation (i.e., the more "realistic" legged model). Our core contribution is advancing the state-of-the-art towards a turn-key approach where the seed values are known by design and do not rely on domain-specific knowledge to generate or randomly guess across a range of energetic cost functions and desired gait properties (e.g., walking speed, hopping height, etc.), which can limit the usefulness of the typical optimization-based approach. We demonstrate this methodology on a parallel elastic actuated planar monoped with five degrees of freedom.**

Our work also demonstrates an explicit connection between passive gaits and optimally actuated motions, which has long been an area of interest in the fields of robotics and biomechanics.

I. Introduction

When trying to understand legged locomotion for highly articulated systems, whether biological or robotic, we often find that energetically conservative models (ECMs) are able to capture the core features of the motion under consideration. For example, the inverted pendulum model describes important features of human walking [1] and the addition of a spring is sufficient to study hopping and running gaits [2]. The influence of these simple models in robotics extend to work in passive dynamic and limit-cycle walking, Raibert-style hoppers, and footstep planning algorithms [3]. Whether the motivation is rooted in biomechanics or robotics, the study of these systems have provided valuable insight into the mechanics of legged locomotion. The passive nature of ECMs makes them particularly interesting in the context of energetic economy.

Specifically, past research on ECMs has demonstrated a relative ease of constructing a variety of gaits at different speeds, inclines, step lengths, or more generally *operating points* of interest of the model. In our recent work, we have presented a methodical approach to generating passive gaits for a general class of ECMs with fixed contact sequences [4]. We have also shown that the passive gaits of simple models of legged systems form continuous sets of gaits that include walking, running, hopping, skipping and galloping motions for elastic bipeds [5], walking and brachiating for compass gait walkers [6] and bounding and galloping for quadrupeds [7]. These passive gaits can be efficiently computed using numerical continuation methods [8] that are seeded with very basic motions such as hopping in place [5] or standing still [9].

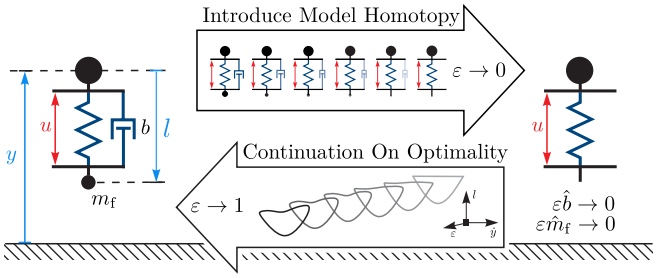

Fig. 1. An illustration of our methodology for a 1D hopper. A model homotopy is introduced by appropriately scaling the damping coefficient b and the foot mass m_f with the parameter ε. $\varepsilon = 1$ yields the full model shown on the left and $\varepsilon = 0$ results in the non-dissipative model shown on the right. The passive hopping gaits (with input $u \equiv 0$) that are found in the model on the right are then traced by numerical continuation methods into optimal active motions of the dissipative model on the left.

In this paper, we present an approach that takes advantage of the ease of finding gaits for ECMs and of the fact that these gaits require zero effort to maintain. We interpret this passivity as an energetic optimum and use the motions as seed values for finding optimal motions of a more realistic robot model. In order to accomplish this task, we introduce a homotopic approach that maps realistic models to their corresponding ECMs and then maps optimal gaits of the ECM back to optimal gaits of the realistic model (Fig. 1). We refer to this parametric scaling as a *model homotopy*.

The mapping between the models is achieved through the appropriate scaling of inertial, damping, and frictional terms so that no energy is lost during the continuous motions or collision events typical of legged robots. To avoid singularities in the dynamics, kinematic constraints are introduced as needed. Given a model homotopy, our contribution is an approach to generating energetically optimal motions that starts with passive gaits for an ECM and mapping this set of optimal gaits to optimal gaits of the target model across various operating points and cost functions without having to guess or intuit seed values to bootstrap the process. We compute optimal gaits using numerical continuation methods, which continuously deforms both the model and resulting motions through our model homotopy.

This approach could be a valuable extension to state-of-the-art optimization-based methods for gait generation [10]–[12]. These optimization-based methods are capable of work-

*This work was funded by the Deutsche Forschungsgemeinschaft (DFG, German Research Foundation) – 501862165. It was further supported through the International Max Planck Research School for Intelligent Systems (IMPRS-IS) for Maximilian Raff and an Alexander von Humboldt fellowship to Nelson Rosa. Additional funding for C. David Remy was provided by the Carl Zeiss Foundation.

[1]The authors are with the Institute for Nonlinear Mechanics, University of Stuttgart, Germany. {raff, nr, remy}@inm.uni-stuttgart.de

2022 IEEE/RSJ International Conference on Intelligent Robots and Systems (IROS) | 978-1-6654-7927-1/22/$31.00 ©2022 IEEE | DOI: 10.1109/IROS47612.2022.9981693

ing with complicated, high-degree-of-freedom robot models. Yet, even the best state-of-the-art frameworks rely to some degree on the user having (or developing) domain-specific knowledge of where to search for optimal gaits with respect to different operating points.

On a more fundamental level, our work is conceptually similar to the notion of templates and anchors [13]. In the context of templates and anchors, our ECM would be considered the template model, while the anchor would be the real robot (i.e., the input model to our framework). Two important distinctions are that we don't necessarily strive for the simplest reduced-order model, and we, by design, map optimal gaits of our template to optimal gaits of the anchor, which in general is an open problem in the work with templates and anchors.

II. Theory

In the following, we provide a formal mathematical description of a model homotopy and establish the necessary assumptions and requirements of our models, controllers, and cost functions.

A. Scaled Dynamics of Legged Systems

In this paper, we consider rigid body systems subject to contact without sliding as they are commonly used to model legged robotic systems. The state of such a system is given by the vector $\boldsymbol{x} = (\boldsymbol{q}, \dot{\boldsymbol{q}}) \in T\mathcal{Q} \subset \mathbb{R}^{2n_\mathrm{q}}$, where $T\mathcal{Q}$ denotes the tangent bundle of the configuration space $\mathcal{Q} \subset \mathbb{R}^{n_\mathrm{q}}$. Hence, the dimension of the robot's configuration $\boldsymbol{q} \in \mathcal{Q}$ reflects the number of its degrees of freedom n_q. The system is driven by an input $\boldsymbol{u} \in \mathbb{R}^{n_\mathrm{u}}$ and the dynamics are scaled by a parameter $\varepsilon \in [0, 1]$, yielding a differential-algebraic equation of the following form:

$$\boldsymbol{M}(\boldsymbol{q}, \varepsilon)\ddot{\boldsymbol{q}} = \boldsymbol{h}(\boldsymbol{x}, \varepsilon) + \boldsymbol{J}_i(\boldsymbol{q}, \varepsilon)^\mathrm{T}\boldsymbol{u} + \boldsymbol{W}_i(\boldsymbol{q})\lambda_i(\varepsilon), \quad \text{(1a)}$$

$$\boldsymbol{g}_i(\boldsymbol{q}) = \boldsymbol{0}, \quad \text{(1b)}$$

with mass matrix $\boldsymbol{M}$ and generalized forces $\boldsymbol{h}$. Since we assume contacts without sliding, the active contacts are reflected in eq. (1b) as holonomic bilateral constraints $\boldsymbol{g}_i$, with constraint Jacobian $\boldsymbol{W}_i(\boldsymbol{q})^\mathrm{T} := \partial \boldsymbol{g}_i / \partial \boldsymbol{q}$ and associated constraint forces λ_i. Hence, the set of constraints (1b) depends on which contacts are active in the current contact configuration (or *phase*). This phase is denoted by $i \in \mathcal{I}$, where $\mathcal{I}$ is the finite set of possible contact configurations. The input Jacobian $\boldsymbol{J}_i^\mathrm{T}$ can be in general also phase dependent to model more complex actuation mechanisms. Phase transitions (i.e., touch-down and lift-off) are triggered by event functions $e_i^j(\boldsymbol{x}, \varepsilon) = 0$, with $e_i^j \in C^2$. The corresponding projection from phase i to j is defined by the discrete map

$$\boldsymbol{\Delta}_i^j(\boldsymbol{x}, \varepsilon) = \begin{bmatrix} \boldsymbol{q} \\ \left(\boldsymbol{I} - \boldsymbol{M}^{-1}\boldsymbol{W}_j\boldsymbol{G}_j^{-1}\boldsymbol{W}_j^\mathrm{T}\right)\dot{\boldsymbol{q}} \end{bmatrix}, \quad (2)$$

where $\boldsymbol{G}_j(\boldsymbol{q}, \varepsilon) = \boldsymbol{W}_j(\boldsymbol{q})^\mathrm{T}\boldsymbol{M}^{-1}(\boldsymbol{q}, \varepsilon)\boldsymbol{W}_j(\boldsymbol{q})$ is known as the Delassus' matrix of phase j [14]. Hence, with $\boldsymbol{x}^+ = \boldsymbol{\Delta}_i^j(\boldsymbol{x}^-, \varepsilon)$, it maps states right before ($\boldsymbol{x}^-$) to states right after ($\boldsymbol{x}^+$) the event e_i^j. Note, this discrete map exclusively depends on the new contact configuration j, which is assumed to be consistent with $\boldsymbol{g}_j(\boldsymbol{q}) = \boldsymbol{0}$.

The scaling with ε is designed such that for $\varepsilon = 0$ all dissipative forces in the generalized torques $\boldsymbol{h}$ (e.g., friction or damping) vanish. Furthermore, masses and inertias in the contact space are scaled, such that as ε approaches zero, $\lim_{\varepsilon \to 0} \boldsymbol{G}_j(\boldsymbol{q}, \varepsilon)^{-1} = \boldsymbol{0}$. This ensures that both the continuous and the discrete dynamics are energetically conservative for $\boldsymbol{u} \equiv \boldsymbol{0}$ (Section III.A in [4]). How such a model design can be achieved is discussed with an example in Section III-A.

We make the following assumptions about the resulting hybrid dynamics so that they are differentiable and have deterministic outcomes post impact:

Assumption (Well-Defined Phase Dynamics)**.** *For each phase $i \in \mathcal{I}$, we assume that*

- *A1 active constraints* (1b) *are independent and consequently, $\boldsymbol{W}_i$ is full rank and the forces λ_i can be uniquely solved for (Theorem 5.1 [14]),*
- *A2 the resulting vector field, defined by eq.* (1)*, is complete for all $\varepsilon \in [0, 1]$ and at least twice differentiable in ε.*

Note, since $\boldsymbol{W}_i$ is full rank (*A1*), the requirement $\lim_{\varepsilon \to 0} \boldsymbol{G}_j(\boldsymbol{q}, \varepsilon)^{-1} = \boldsymbol{0}$ yields a singular mass matrix $\boldsymbol{M}(\boldsymbol{q}, 0)$ [4]. However, as discussed in Section III.A in [4], an appropriate ε-scaling of eq. (1a) yields finite and well defined accelerations $\ddot{\boldsymbol{q}}$ even in the limit $\varepsilon \to 0$ (*A2*).

Assumption (Fixed Phase Sequence)**.** *We assume that the phase sequence of a hybrid flow $\boldsymbol{x}(t)$ is a priori known and is fixed under local changes of the initial time t_0, initial state $\boldsymbol{x}_0$, parameter ε, and control inputs $\boldsymbol{u}$.*

This assumption allows us to assign the total number of phases $m \in \mathbb{N}$ to a hybrid flow $\boldsymbol{x}(t)$, where $\boldsymbol{t} = [t_1 \dots t_m]^\mathrm{T}$ collects the duration of each phase that $\boldsymbol{x}(t)$ passes through.

B. Input Parameterization

To simplify the optimal control problem, we parameterize the function space of the input $\boldsymbol{u}(\cdot)$ by the control parameters $\boldsymbol{\xi} \in \mathbb{R}^{n_\xi}$, with $n_\xi \in \mathbb{N}_{\geq 2}$, such that $\boldsymbol{u} : \mathbb{R} \times T\mathcal{Q} \times \mathbb{R}^{n_\xi} \to \mathbb{R}^{n_\mathrm{u}}$.

Assumption (Input Parameterization)**.** *The parameterization of the input function is such that*

$$\boldsymbol{u} \in C^2, \quad (3)$$

$$\boldsymbol{u}(t, \boldsymbol{x}, \boldsymbol{0}) \equiv \boldsymbol{0}, \quad (4)$$

$$\boldsymbol{u}(t, \boldsymbol{x}, \boldsymbol{\xi}^*) = \boldsymbol{u}(t, \boldsymbol{x}, \boldsymbol{\xi}^{**}) \Rightarrow \boldsymbol{\xi}^* = \boldsymbol{\xi}^{**}, \quad (5)$$

for all $t \in \mathbb{R}$, $\boldsymbol{x} \in T\mathcal{Q}$ and $\boldsymbol{\xi} \in \mathbb{R}^{n_\xi}$.

Remark II.1. *Eq.* (5) *is equivalent to the requirement of linearly independent basis functions in $\boldsymbol{u}(\cdot)$ as they are found in Bézier curves, B-Splines [15] and Fourier series. With these basis functions, eq.* (4) *is also satisfied.*

Remark II.2. *The input is in the class of parameterized open-loop functions if $\boldsymbol{u} = \boldsymbol{u}(t, \boldsymbol{\xi})$ does not depend on the state, and in the class of parameterized feedback controllers if $\boldsymbol{u} = \boldsymbol{u}(\boldsymbol{x}(t), \boldsymbol{\xi})$ (i.e., not explicitly dependent on t).*

Under a fixed phase sequence, the Assumptions *A1*, *A2* and the input parameterization yield a unique non-autonomous flow $\boldsymbol{x}(t) = \boldsymbol{\varphi}(t, t_0, \boldsymbol{x}_0; \boldsymbol{\xi}, \varepsilon)$, with initial time t_0 and initial state $\boldsymbol{x}_0$. Furthermore, the flow is at least twice differentiable with respect to t_0, $\boldsymbol{x}_0$, $\boldsymbol{\xi}$ and ε. For $\varepsilon = 0$ and $\boldsymbol{\xi} = \mathbf{0}$, this flow is energetically conservative. That is, if $E : T\mathcal{Q} \to \mathbb{R}$ denotes the total energy in the systems, it holds:

$$E(\boldsymbol{\varphi}(t, t_0, \boldsymbol{x}_0; \mathbf{0}, 0)) = const., \quad \forall t, t_0 \in \mathbb{R}, \forall \boldsymbol{x}_0 \in T\mathcal{Q}.$$

C. Periodic Gaits

For this system, we are interested in periodic flows with period time $T > 0$ and a constant matrix $\boldsymbol{A}_\mathrm{p}$ such that $\boldsymbol{A}_\mathrm{p} \cdot (\boldsymbol{x}(T) - \boldsymbol{x}_0) = \mathbf{0}$. This notion of periodicity results from the fact that gaits of legged systems are not necessarily periodic in all states. In particular, the horizontal position is aperiodic to allow for forward motion. Hence, we split the state $\boldsymbol{x}$ into a periodic part $\boldsymbol{x}_\mathrm{p} := \boldsymbol{A}_\mathrm{p}\boldsymbol{x}$ and a non-periodic part $\boldsymbol{x}_\mathrm{np} := \boldsymbol{A}_\mathrm{np}\boldsymbol{x}$ by introducing the constant orthonormal selection matrix $\boldsymbol{A}_\mathrm{s} = \begin{bmatrix} \boldsymbol{A}_\mathrm{p} \\ \boldsymbol{A}_\mathrm{np} \end{bmatrix} \in \mathbb{R}^{2n_\mathrm{q} \times 2n_\mathrm{q}}$ [4]. In addition to this periodicity constraint, we introduce two C^2 functions $a : T\mathcal{Q} \to \mathbb{R}$ and $O : T\mathcal{Q} \times \mathbb{R}^m \times \mathbb{R}^{n_\xi} \times \mathbb{R} \to \mathbb{R}$ that encode two additional gait specifications. With the first, we introduce an anchor constraint $a(\boldsymbol{x}_0) = 0$. This anchor could, for example, encode the requirement that a stride always starts at apex transit. With the second, we introduce an additional implicit function $O(\boldsymbol{x}_0, \boldsymbol{t}, \boldsymbol{\xi}, \bar{O}) = 0$ that restricts the motion to a given operating point $\bar{O}$. With this function we can require, for example, that the resulting gait has a desired average speed, a certain stride time, or is on a given energy level.

Putting all this together, a periodic motion (or *gait*) is determined by the roots of the function $\mathbf{h}(\boldsymbol{x}_0, \boldsymbol{t}, \boldsymbol{\xi}, \bar{O}, \varepsilon) = \mathbf{0}$:

$$\mathbf{h}(\cdot) = \begin{bmatrix} \boldsymbol{A}_\mathrm{p} \cdot (\boldsymbol{\varphi}(t_m, t_{m-1}, \boldsymbol{x}_{0,m}; \boldsymbol{\xi}, \varepsilon) - \boldsymbol{x}_0) \\ \boldsymbol{A}_\mathrm{np} \cdot \boldsymbol{x}_0 \\ e^m_{m-1}\left(\boldsymbol{\varphi}\left(t_{m-1}, t_{m-2}, \boldsymbol{x}_{0,m-1}; \boldsymbol{\xi}, \varepsilon\right), \varepsilon\right) \\ \vdots \\ e^2_1\left(\boldsymbol{\varphi}\left(t_1, t_0, \boldsymbol{x}_{0,1}; \boldsymbol{\xi}, \varepsilon\right), \varepsilon\right) \\ a(\boldsymbol{x}_0) \\ O(\boldsymbol{x}_0, \boldsymbol{t}, \boldsymbol{\xi}, \bar{O}) \end{bmatrix}, \quad (6)$$

where the period results from $T = \sum_{i=0}^{m} t_i$, with $t_0 = 0$, and the initial states of each phase are defined recursively:

$$\boldsymbol{x}_{0,i} = \boldsymbol{\Delta}^i_{i-1} \circ \boldsymbol{\varphi}\left(t_{i-1}, t_{i-2}, \boldsymbol{x}_{0,i-1}; \boldsymbol{\xi}, \varepsilon\right), \quad \boldsymbol{x}_{0,1} = \boldsymbol{x}_0.$$

Note that for a root of eq. (6) all phase times t_i, with $i > 0$, are implicitly defined by events e^{i+1}_i and the anchor a.

A notable subset of the gaits defined by eq. (6) are passive gaits that have neither actuation nor losses:

Definition (Passive Gait)**.** *A passive gait is given by a root $(\boldsymbol{x}_0, \boldsymbol{t}, \boldsymbol{\xi}, \bar{O}, \varepsilon) \in \mathbf{h}^{-1}(\mathbf{0})$, where $\varepsilon = 0$ and $\boldsymbol{\xi} = \mathbf{0}$.*

Passive gaits are periodic solutions of autonomous energetically conservative systems, and hence the definition above is equivalent to a root of eq. (20) in [4], where it is shown that the passive gaits form 1D families of connected periodic motions. These families are here parameterized by the operating point $\bar{O}$, which is a generalization of the parameterization by energy level $\bar{E}$ in [4]. By doing a numerical continuation on eq. (6), the passive gaits can be efficiently computed for a range of operating points $\bar{O}$. This continuation approach is initialized with very basic motions such as hopping in place or standing still. The algorithmic details of this process can be found in [4]. In this work, we will use the passive gaits as templates for energetically optimal active motions.

D. Optimally Actuated Gaits

To this end, let us relax the requirement that $\boldsymbol{\xi} = \mathbf{0}$ while we continue to consider the non-dissipative model (i.e., $\varepsilon = 0$). In this case, many different gaits with different input parameterizations $\boldsymbol{\xi}$ can be found as solutions for eq. (6), but energy may not be conserved. Of course, the passive gaits with $\boldsymbol{\xi} = \mathbf{0}$ continue to be solutions, and since they come with zero effort ($\boldsymbol{u}(\cdot) \equiv \mathbf{0}$) they can be interpreted as optimal for a wide range of effort-based cost functions. In the following, we formalize this idea and show that for suitable cost functions the passive gaits are actually *strict* minimas of such an optimization problem.

Definition (Energetic Cost Functions)**.** *Listed as follows, we consider energetic cost functions of the form $\mathsf{f} : T\mathcal{Q} \times \mathbb{R}^m \times \mathbb{R}^{n_\xi} \times [0, 1] \to \mathbb{R}$ that are*

C1 at least twice differentiable in all variables, i.e., $\mathsf{f} \in C^2$,
C2 of zero value when $\boldsymbol{u}(\cdot) \equiv \mathbf{0}$ and $\varepsilon = 0$, i.e., $\mathsf{f}(\boldsymbol{x}_0, \boldsymbol{t}, \mathbf{0}, 0) = 0$, and
C3 locally positive-definite in $\frac{\partial^2 \mathsf{f}}{\partial \boldsymbol{\xi}^2}(\boldsymbol{x}_0, \boldsymbol{t}, \boldsymbol{\xi}, \varepsilon)\big|_{(\boldsymbol{\xi}=\mathbf{0}, \varepsilon=0)}$.

Remark II.3. *For passive gaits, the properties C1 - C3 are within a wide class of energetic costfunctions for robotic systems including the integral of the square of actuator forces, thermal electrical losses, positive mechanical actuator work and positive electrical work [16]. Herein, smoothing may be required to meet C1.*

Remark II.4. *The choice of mechanical actuator work, with $\mathsf{f} = \int_0^T \dot{\boldsymbol{q}}^\mathrm{T} \boldsymbol{u} \, \mathrm{d}t$, does not satisfy C3 as f remains zero in the neighborhood of a passive gait where $\boldsymbol{u}(\cdot) \neq \mathbf{0}$ injects and removes the same amount of energy.*

To properly couple the energetic cost function f with the constitutive gait constraints (6), we define the constrained optimization problem (COP):

$$\mathrm{COP}(\bar{O}, \varepsilon) = \begin{cases} \underset{\mathsf{x}}{\text{minimize}} & \mathsf{f}\left(\mathsf{x}, \varepsilon\right) \\ \text{subject to} & \mathbf{h}\left(\mathsf{x}, \bar{O}, \varepsilon\right) = \mathbf{0}, \end{cases}$$

where $\mathsf{x}^\mathrm{T} = [\boldsymbol{x}_0^\mathrm{T} \ \boldsymbol{t}^\mathrm{T} \ \boldsymbol{\xi}^\mathrm{T}] \in \mathbb{R}^{2n_\mathrm{q}+m+n_\xi}$. We can state the first-order condition for $\mathrm{COP}(\bar{O}, \varepsilon)$ as

$$\frac{\partial \mathsf{f}}{\partial \mathsf{x}}(\mathsf{x}, \varepsilon) + \boldsymbol{\lambda}^\mathrm{T} \frac{\partial \mathbf{h}}{\partial \mathsf{x}}(\mathsf{x}, \bar{O}, \varepsilon) = \mathbf{0}, \quad (7)$$

with Lagrange multipliers $\boldsymbol{\lambda} \in \mathbb{R}^{2n_\mathrm{q}+m+1}$. The existence and uniqueness of $\boldsymbol{\lambda}$ directly follows from $\mathbf{x}$ being a local extremum point of f subject to the constraints $\mathbf{h}(\cdot) = \mathbf{0}$ and $\partial\mathbf{h}/\partial\mathbf{x}$ having full rank (Chapter 11.3 [17]).

Definition (Regular Point)**.** *We call a solution $\boldsymbol{\gamma}^*$ of an implicit function $\boldsymbol{r} : \mathbb{R}^{n_1} \to \mathbb{R}^{n_2}$ with $\boldsymbol{r}(\boldsymbol{\gamma}^*) = \mathbf{0}$ a regular point if $(\partial\boldsymbol{r}/\partial\boldsymbol{\gamma})|_{\boldsymbol{\gamma}=\boldsymbol{\gamma}^*}$ has maximum rank.*

Furthermore, a regular point $(\mathbf{x}^*, \bar{O}, \varepsilon)$ of eq. (6), with $(\bar{O}, \varepsilon)$ being fixed, allows us to define the tangent space in $\mathbf{x}^*$ as $\mathsf{M} = \{\mathbf{y} : (\partial\mathbf{h}/\partial\mathbf{x})|_{\mathbf{x}=\mathbf{x}^*}\mathbf{y} = \mathbf{0}\}$. The second-order condition can thus be stated as

$$\mathbf{y}^\mathrm{T}\Bigg(\underbrace{\frac{\partial^2\mathsf{f}}{\partial\mathbf{x}^2}(\mathbf{x},\varepsilon) + \boldsymbol{\lambda}^\mathrm{T}\frac{\partial^2\mathbf{h}}{\partial\mathbf{x}^2}(\mathbf{x},\bar{O},\varepsilon)}_{=:\mathsf{H}}\Bigg)\mathbf{y} > 0, \quad \forall\mathbf{y} \in \mathsf{M}. \quad (8)$$

Remark II.5. *The first-order condition* (7) *is only a necessary optimality condition, since $COP(\bar{O}, 0)$ is in general nonconvex. Hence, the second-order condition* (8) *is sufficient for a stationary point to be also a strict local minimizer.*

From conditions (7) and (8) we see that regularity of the COP's equality constraints is crucial to identify a strict local minimum (Chapter 11.5 [17]). This also becomes important for (optimal) passive gaits, since regularity can be lost when passive gaits bifurcate into another family of gaits or lie on turning points with respect to the parameterization $\bar{O}$ [4]. Hence, passive gaits are strict minimizers $(\boldsymbol{x}_\mathbf{0}, \boldsymbol{t}, \mathbf{0})$ of $\mathrm{COP}(\bar{O}, 0)$ only if they are regular points of eq. (6).

Lemma II.1. *A passive gait $\mathbf{x}^* = (\boldsymbol{x}_0^*, \boldsymbol{t}^*, \boldsymbol{\xi}^*)$, with $\boldsymbol{\xi}^* = \mathbf{0}$, that is a regular point at an operating point $\bar{O}$ of eq.* (6)*, is a strict minimizer of $COP(\bar{O}, 0)$ and thus, fulfills the first- and second-order optimality conditions.*

Proof. Since the regular point $\mathbf{x}^*$ is isolated from other passive gaits, only a nonzero $\boldsymbol{u}(\cdot)$ leads to different gaits in its neighborhood (i.e., roots of the constraint (6)). Nonzero actuation can only be achieved for an arbitrary $\boldsymbol{\xi} \neq \mathbf{0}$ due to the assumption in eq. (5). Hence, as any change in $\boldsymbol{\xi}$ will lead to an increase in the value of f (*C3*), the passive gait corresponding to $\mathbf{x}^*$ is the only local solution to eq. (6) with zero cost (*C2*). □

E. Continuation of First-Order Optimality

Now that we have established that passive gaits can be interpreted as optimally actuated gaits within a non-dissipative model, we trace these optimal gaits throughout the model homotopy (Fig. 1). For notational convenience, the first-order conditions in eq. (6) and eq. (7) can be generalized as $\partial/\partial\mathbf{z}\mathsf{L}(\mathbf{z}, \bar{O}, \varepsilon) = \mathbf{0}$, with the Lagrangian

$$\mathsf{L}(\mathbf{z}, \bar{O}, \varepsilon) = \mathsf{f}(\mathbf{x}, \varepsilon) + \boldsymbol{\lambda}^\mathrm{T}\mathbf{h}(\mathbf{x}, \bar{O}, \varepsilon), \quad (9)$$

and the vector $\mathbf{z}^\mathrm{T} = [\mathbf{x}^\mathrm{T}\ \boldsymbol{\lambda}^\mathrm{T}]$.

Remark II.6. *With the aforementioned differentiability conditions on f and $\mathbf{h}$, the Lagrangian $\mathsf{L}(\mathbf{z}, \bar{O}, \varepsilon)$ is also at least twice differentiable in all its variables.*

Algorithm 1: Continuation on First-Order Optimality

Input: Regular passive gait $\mathbf{x}^*$ with $\varepsilon^* = 0$ and fixed $\bar{O}$; Step size $h > 0$
Output: Stationary point $\boldsymbol{\gamma} = (\mathbf{z}, 1)$

uniquely solve for $\boldsymbol{\lambda}^*$ /* eq. (7) */
$\boldsymbol{\gamma}^* = (\mathbf{z}^*, \varepsilon^*)$ with $\mathbf{z}^* = (\mathbf{x}^*, \boldsymbol{\lambda}^*)$
compute initial tangent vector $\boldsymbol{p}^*$ /* eq. (10) */
$d_\mathrm{p} = \mathrm{sign}(p^*_\mathrm{end})$ /* orientation of curve */
$\boldsymbol{\gamma} \leftarrow \boldsymbol{\gamma}^*$, $\boldsymbol{p} \leftarrow \boldsymbol{p}^*$, $\varepsilon \leftarrow \varepsilon^*$
while $\varepsilon < 1$ **do**
  $\boldsymbol{\gamma}_\mathrm{pred} \leftarrow \boldsymbol{\gamma} + d_\mathrm{p} h \boldsymbol{p}$ /* predictor step */
  compute $\boldsymbol{p}_\mathrm{pred}$ at $\boldsymbol{\gamma}_\mathrm{pred}$ /* eq. (10) */
  Newton's Method $(\boldsymbol{\gamma}_\mathrm{pred}, \boldsymbol{p}_\mathrm{pred})$**:**
    $\boldsymbol{\gamma} \leftarrow \boldsymbol{\gamma} - \begin{bmatrix} \boldsymbol{R}(\boldsymbol{\gamma}) \\ \boldsymbol{p}^\mathrm{T} \end{bmatrix}^{-1} \cdot \begin{bmatrix} \boldsymbol{r}(\boldsymbol{\gamma}) \\ 0 \end{bmatrix}$ /* corrector */
    until convergence /* loop */
    return $\{\boldsymbol{\gamma}_\mathrm{corr} = (\mathbf{z}_\mathrm{corr}, \varepsilon_\mathrm{corr});\ \boldsymbol{p}_\mathrm{corr}\}$
  $\boldsymbol{\gamma} \leftarrow \boldsymbol{\gamma}_\mathrm{corr}$, $\boldsymbol{p} \leftarrow \boldsymbol{p}_\mathrm{corr}$, $\varepsilon \leftarrow \varepsilon_\mathrm{corr}$
check 2nd-order optimality of $\boldsymbol{\gamma} = (\mathbf{z}, 1)$ /* eq. (8) */

We use the subscript notation $\mathsf{L}_{\bar{O}}(\mathbf{z}, \varepsilon)$ and $\mathsf{L}_{\varepsilon}(\mathbf{z}, \bar{O})$ to emphasize the fixed parameters $\bar{O}$ and ε in eq. (9), respectively. For a given passive gait defined by a regular point $(\boldsymbol{x}_0, \boldsymbol{t}, \mathbf{0}, \bar{O}, 0)$, the stationary condition of eq. (9) can now be traced into a unique direction of increasing ε.

Proposition (Regularity of First-Order Optimality)**.** *A passive gait $(\mathbf{x}^*, \varepsilon = 0)$ that is a regular point of eq.* (6) *at $\bar{O}$, is also a regular point of $\partial/\partial\mathbf{z}\mathsf{L}_{\bar{O}}(\mathbf{z}, \varepsilon) = \mathbf{0}$.*

Proof. Due to Lemma II.1, $\mathbf{x}^*$ is a strict local minimizer and $\boldsymbol{\lambda}^*$ is uniquely given by eq. (7). This implies that for a fixed $\varepsilon = 0$, the point $\mathbf{z}^{*\mathrm{T}} = [\mathbf{x}^{*\mathrm{T}}\ \boldsymbol{\lambda}^{*\mathrm{T}}]$ is isolated in the solution space of $\partial/\partial\mathbf{z}\mathsf{L}_{\bar{O}}(\mathbf{z}, \varepsilon) = \mathbf{0}$ and thus, the square matrix $\partial^2/\partial\mathbf{z}^2\mathsf{L}_{\bar{O}}|_{(\mathbf{z}^*,0)}$ is regular. Hence, $(\mathbf{z}^*, 0)$ is a regular point since

$$\frac{\partial}{\partial(\mathbf{z},\varepsilon)}\left(\frac{\partial\mathsf{L}_{\bar{O}}}{\partial\mathbf{z}}\right)\Bigg|_{(\mathbf{z}^*,0)} = \begin{bmatrix} \dfrac{\partial^2\mathsf{L}_{\bar{O}}}{\partial\mathbf{z}^2}\Big|_{(\mathbf{z}^*,0)} & \dfrac{\partial^2\mathsf{L}_{\bar{O}}}{\partial\varepsilon\partial\mathbf{z}}\Big|_{(\mathbf{z}^*,0)} \end{bmatrix}$$

has maximum (row) rank. □

With the homotopy map $\boldsymbol{r}(\mathbf{z}, \varepsilon) := \partial/\partial\mathbf{z}\mathsf{L}_{\bar{O}}(\mathbf{z}, \varepsilon)$ for a fixed $\bar{O}$, we define a sequence of root-finding problems in ε that is solved by a pseudo-arclength continuation (Chapter 6.1 [8]). Algorithm 1 employs a predictor-corrector (PC) method which takes small iterative steps in the tangent space of $\boldsymbol{r}(\mathbf{z}, \varepsilon) = \mathbf{0}$ to locally trace the solution curve $\boldsymbol{\gamma}$ of regular points. The tangent vector $\boldsymbol{p}$ at a regular point $(\mathbf{z}^*, \varepsilon^*)$ is uniquely defined by

$$\underbrace{\frac{\partial\boldsymbol{r}(\mathbf{z},\varepsilon)}{\partial(\mathbf{z},\varepsilon)}\Big|_{(\mathbf{z}^*,\varepsilon^*)}}_{=:\boldsymbol{R}(\mathbf{z},\varepsilon)} \cdot \boldsymbol{p} = \mathbf{0}, \quad (10a)$$

$$\|\boldsymbol{p}\|_2 = 1, \qquad \det\left(\begin{bmatrix} \boldsymbol{R}(\mathbf{z}^*,\varepsilon^*) \\ \boldsymbol{p}^\mathrm{T} \end{bmatrix}\right) > 0. \quad (10b)$$

Initially, the orientation d_p of the solution curve should correspond to an increase of ε. Therefore, we set $d_\mathrm{p} = \mathrm{sign}(p^*_\mathrm{end})$, where p^*_end is the last entry of the tangent vector $\boldsymbol{p}^*$ at the

regular point $\boldsymbol{\gamma}^* = \boldsymbol{\gamma}(\mathbf{z}^*, 0)$. Note, p^*_{end} is always nonzero initially, since regular passive gaits do not correspond to a turning point in ε (see proof of Proposition (Regularity of First-Order Optimality)). Algorithm 1 is terminated when ε crosses the value of one. Since we only trace gaits from the template to anchor (Fig. 1) that meet the necessary first-order condition (7), it remains to confirm the sufficient condition (8) for $\mathrm{COP}(\bar{O}, 1)$.

III. Example: Two-Dimensional Monoped

To demonstrate the applicability of these methods, we generate optimally actuated gaits for a 2D one-legged hopping robot with parallel elastic actuation (Fig. 2), as it has been the subject of study in [16], [18], [19]. To this end, we develop a suitable model homotopy in ε, and define a constrained optimization problem by choosing a cost function, an input parameterization, and a set of operating points.

The hopper consists of a torso with mass m_{t} and inertia Θ_{t}, an upper leg segment $(m_{\mathrm{l}}, \Theta_{\mathrm{l}})$, and a lower leg segment $(m_{\mathrm{f}}, \Theta_{\mathrm{f}})$ with a spherical foot (radius r_{f}). The torso's configuration is given by the orientation φ and the hip position (x, y). On its proximal end, the upper leg segment is connected to the hip via a rotational joint (with joint angle α) and on the distal end it is connected to the lower leg with a prismatic joint (overall leg length of l). Thus, the generalized coordinates are $\boldsymbol{q} = [x\ y\ \varphi\ \alpha\ l]^{\mathrm{T}}$, with $n_{\mathrm{q}} = 5$. In both joints, linear elastic springs (with stiffnesses k_α, k_{l} and damping ratios b_α, b_{l}) are mounted in parallel to actuators that produce the torques $\boldsymbol{u} = [\tau_{\mathrm{mot}}\ f_{\mathrm{mot}}]^{\mathrm{T}}$. The remaining model parameters are defined in Fig. 2 and Table I. All values have been normalized with respect to total mass m_o, leg length l_o and gravity g. The hopper has two phases: *stance* S and *flight* F. During *stance*, the foot stays on the ground and is constrained to a pure rolling motion $\boldsymbol{g}_{\mathrm{S}}(\boldsymbol{q}) = 0$ with the associated constraint forces $\boldsymbol{\lambda}_{\mathrm{S}} = [\lambda_{\mathrm{T}}\ \lambda_{\mathrm{N}}]^{\mathrm{T}}$.

A. Model Homotopy

To create the model homotopy, we start with a standard multibody dynamic model of the hopper. This model constitutes the dynamics for $\varepsilon = 1$. Since it includes damping and collision losses, we follow a similar approach as the one reported in IV.A [4] to yield a non-dissipative model for $\varepsilon = 0$. In order to bring $\lim_{\varepsilon\to 0} \boldsymbol{G}_{\mathrm{S}}(\boldsymbol{q}, \varepsilon)^{-1}$ to zero, we scale the masses and inertias m_{f}, m_{l}, Θ_{f}, Θ_{l} which are involved in the projection $\boldsymbol{G}_{\mathrm{S}}$. This is achieved by redefining the foot and leg mass with $m_{\mathrm{f}} = \varepsilon \hat{m}_{\mathrm{f}}$ and $m_{\mathrm{l}} = \varepsilon \hat{m}_{\mathrm{l}}$, respectively. Due to this scaling, the inertial torques originating from the leg will vanish for $\varepsilon \to 0$. In order to maintain meaningful pitch dynamics, we thus also have to scale the torso inertia with $\Theta_{\mathrm{t}} = \varepsilon \hat{\Theta}_{\mathrm{t}}$. The degrees of freedom describing the massless limbs need to be constrained in all phases to meet *A2* [4], [20]. Hence, we introduce the *flight* constraint $g_{\mathrm{F}}(\boldsymbol{q}) = l - l_o$ with constraint force λ_{F}. Similar to [4], we introduce new auxiliary forces $\hat{\lambda}_{\mathrm{F}}$ and $\hat{\boldsymbol{\lambda}}_{\mathrm{S}}$ in the constraint forces $\lambda_{\mathrm{F}}(\varepsilon) = \varepsilon \hat{\lambda}_{\mathrm{F}}$ and $\boldsymbol{\lambda}_{\mathrm{S}}(\varepsilon) = \varepsilon \hat{\boldsymbol{\lambda}}_{\mathrm{S}}$, respectively. Additionally, since $g_{\mathrm{F}}(\boldsymbol{q}) = 0$ is only needed for $\varepsilon = 0$, we multiply the resulting constraint force λ_{F} with $(1 - \varepsilon)$ when we include it in eq. (1a). Similarly to eq. (18) in [4], we scale the spring stiffness in the hip ($k_\alpha = \varepsilon \hat{k}_\alpha$) to yield a finite leg swing frequency for $\varepsilon \to 0$. Since the damping force $b_\alpha \dot{\alpha}$ and the actuation $\boldsymbol{u}$ would experience a similar singularity, we further introduce the scaling:

$$\boldsymbol{J}_i = \begin{bmatrix} 0 & 0 & 0 & \varepsilon & 0 \\ J_i^{21} & J_i^{22} & 0 & 0 & \varepsilon \end{bmatrix}, \quad b_\alpha = \varepsilon^2 \hat{b}_\alpha, \tag{11}$$

where $J_{\mathrm{F}}^{21} = J_{\mathrm{F}}^{22} = 0$, $J_S^{21} = -\sin(\alpha + \varphi)(1 - \varepsilon)$ and $J_i^{22} = \cos(\alpha + \varphi)(1 - \varepsilon)$. Herein, the repeated multiplication of the damping $\hat{b}_\alpha$ by ε results from the final scaling law: in order to remove damping losses in eq. (1) for $\varepsilon \to 0$, we simply scale the damping coefficients with ε. Similarly, we set $b_{\mathrm{l}} = \varepsilon \hat{b}_{\mathrm{l}}$.

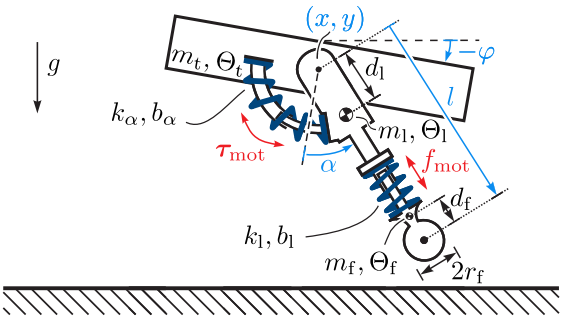

Fig. 2. A one-legged hopper with parallel elastic actuation in the leg and hip joint ($\boldsymbol{u} = [\tau_{\mathrm{mot}}\ f_{\mathrm{mot}}]^{\mathrm{T}}$). Its planar configuration is described by $\boldsymbol{q} = [x\ y\ \varphi\ \alpha\ l]^{\mathrm{T}}$.

m_{f}	$= 0.1\ m_o$	k_{l}	$= 20\ m_o g / l_o$	r_{f}	$= 0.05\ l_o$
m_{l}	$= 0.2\ m_o$	k_α	$= 100\ m_{\mathrm{f}} g l_o / \mathrm{rad}$	d_{l}	$= 0.25\ l_o$
m_{t}	$= 0.7\ m_o$	b_{l}	$= 0.4\sqrt{2}\ m_o \sqrt{g/l_o}$	d_{f}	$= 0.25\ l_o$
Θ_{f}	$= 0.04\ m_{\mathrm{f}} l_o^2$	b_α	$= 3.5\ m_{\mathrm{f}} l_o \sqrt{g l_o} / \mathrm{rad}$		
Θ_{l}	$= 0.02\ m_{\mathrm{l}} l_o^2$				
Θ_{t}	$= 0.40\ m_{\mathrm{t}} l_o^2$				

TABLE I

All model parameters are taken from [18] and normalized with respect to total mass m_o, leg length l_o and gravity g.

B. Results

For this model, we generated optimal gaits at different average forward velocities $\dot{x}_{\mathrm{avg}} := \bar{O}$. To this end, we defined $O(\boldsymbol{x}_0, \boldsymbol{t}, \boldsymbol{\xi}, \dot{x}_{\mathrm{avg}}) := x(T) - x(0) - \dot{x}_{\mathrm{avg}} T$, where $x(0)$ and $x(T)$ are extracted from the initial conditions and the flow, respectively. We further restricted all motions to the phase sequence S $\to$ F, which is started right after the touchdown event $e_{\mathrm{F}}^{\mathrm{S}}(\boldsymbol{q}) = [0\ 1] \cdot \boldsymbol{g}_{\mathrm{S}}(\boldsymbol{q})$. This event takes on the role of the anchor constraint a, which thus can be dropped in the implementation of eq. (6). To allow for a horizontal forward motion during the gait, the matrix $\boldsymbol{A}_{\mathrm{np}}$ in eq. (6) selects the initial state $x_0 = \boldsymbol{A}_{\mathrm{np}} \boldsymbol{x}_0$ (i.e., $\boldsymbol{A}_{\mathrm{np}} = [1\ 0 \cdots 0]$). The remaining periodic states are selected by its orthogonal complement $\boldsymbol{A}_{\mathrm{p}}$. While $e_{\mathrm{F}}^{\mathrm{S}}(\boldsymbol{q})$ was defined kinematically, the lift-off event $e_{\mathrm{S}}^{\mathrm{F}}(\boldsymbol{x}, \varepsilon) = \boldsymbol{\lambda}_{\mathrm{N}}$ is triggered when $\boldsymbol{\lambda}_{\mathrm{N}}$ changes sign from positive to negative. For $\boldsymbol{u} = [\tau_{\mathrm{mot}}\ f_{\mathrm{mot}}]^{\mathrm{T}}$, we

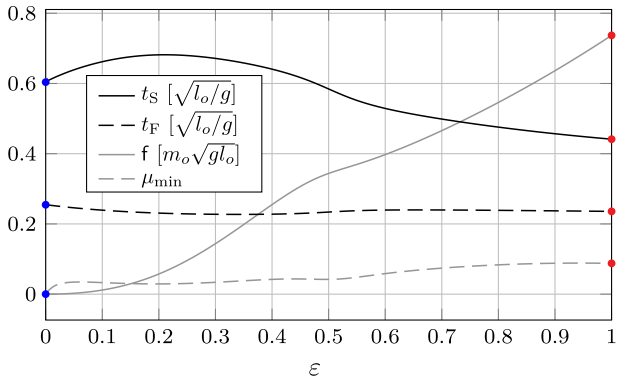

Fig. 3. Shown is the evolution of the stance time t_S, the flight time t_F, the cost value f and $\mu_{\min}$ in the transition from the non-dissipative model at $\varepsilon = 0$ (blue) to the full model at $\varepsilon = 1$ (red). The value of the smallest eigenvalue of the projected Hessian matrix $\mathbf{H}_M$ at $\varepsilon = 0$ is $\mu_{\min}(0) = 0.005$. It always remains positive, indicating that the motion remains strictly optimal throughout the homotopy. This data is from a forward hopping motion with $\dot{x}_{\text{avg}} = 1\ \sqrt{gl_o}$. All values have been normalized with respect to total mass m_o, leg length l_o and gravity g.

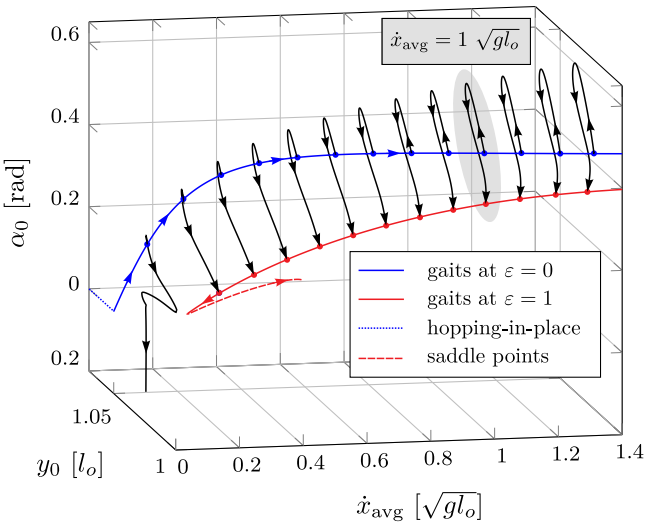

Fig. 4. Shown is a projection of the space of initial states (α_0 and y_0). Passive gaits (shown in blue) with f $= 0$, $\boldsymbol{u} \equiv \mathbf{0}$, have been identified via numerical continuation that was started from a passive hopping-in-place motion. By applying a model homotopy, these gaits have been traced from $\varepsilon = 0$ into locally optimal solutions of the model at $\varepsilon = 1$ (shown in red). A different continuation with a fixed $\varepsilon = 1$ (red line) reveals a turning point at $\dot{x}^*_{\text{avg}} \approx 0.12\ \sqrt{gl_o}$, at which the stationary points become saddle points and are thus no longer optimal gaits.

choose a 3-term Fourier series ($n_\xi = 14$):

$$\boldsymbol{u}(\cdot) = \boldsymbol{\xi}_0 + \sum_{k=1}^{3} \left(\boldsymbol{\xi}_{2k-1} \cos\left(\frac{2\pi}{T} kt\right) + \boldsymbol{\xi}_{2k} \sin\left(\frac{2\pi}{T} kt\right) \right),$$

Finally, we used torque-squared as cost function: $\text{f} = \int_0^T \boldsymbol{u}(\cdot)^{\mathrm{T}} \boldsymbol{u}(\cdot)\, \mathrm{d}t$, for which *C1-C3* are easy to confirm.

Using these choices and the methods described in [4], we first explored the connected space of passive gaits. This search was initialized with a simple hopping-in-place motion that was derived analytically. Due to different parameter choices, our non-dissipative model had a much larger leg swing frequency than the model used in [5]. In contrast to the results reported in [5], we thus found the first bifurcation that connected the hopping-in-place branch with forward/backward hopping motions at a significantly smaller *flight* time of $t_F \approx 0.1658\ \sqrt{g/l_o}$. Subsequently, the branch of passive forward hopping motions was identified for average speeds of up to $\dot{x}_{\text{avg}} = 1.4\ \sqrt{gl_o}$.

Algorithm 1 was initialized with these motions and the first-order optimality was successfully traced from the passive gaits of the non-dissipative model ($\varepsilon = 0$) to the desired optimally actuated gaits of the model at $\varepsilon = 1$. For $\dot{x}_{\text{avg}} = 1\ \sqrt{gl_o}$, this process is illustrated in Figure 3 and visualized in the multimedia extension[1]. In the transition from $\varepsilon = 0$ to $\varepsilon = 1$, the cost f is monotonically increasing from 0 to $0.737\ m_o g \sqrt{gl_o}$. Throughout the model homotopy, the motion remained optimal. That is, not only the first-order optimality conditions are fulfilled, but also the second-order conditions (8). This can be shown by the projected Hessian matrix $\mathbf{H}_M$ which projects $\mathbf{H}$ onto the tangent space M. From this, we can readily compute its eigenvalues $\boldsymbol{\mu}$. Herein, the smallest eigenvalue $\mu_{\min}$ has to be greater than zero to satisfy the sufficient condition (Chapter 11.6 [17]). This eigenvalue is also illustrated in Fig. 3.

We repeated this process for a range of other forward speeds $\dot{x}_{\text{avg}}$ between 0 and $1.4\ \sqrt{gl_o}$, always using the passive gaits as the starting point. This process always converged for speeds larger than $\dot{x}^*_{\text{avg}} \approx 0.12\ \sqrt{gl_o}$. For a number of selected forward speeds, it is illustrated in a projection of the space of initial states $\boldsymbol{x}_0$ in Fig. 4. In this figure, the branch of passive forward hopping gaits is shown as a red line, emerging from the family of hopping-in-place motions (red dashed line), while the active gaits of the full model are shown as blue dots. The connecting black lines show how $\boldsymbol{x}_0$ changes throughout the homotopy.

To understand why the process failed for speeds smaller than $\dot{x}^*_{\text{avg}} \approx 0.12\ \sqrt{gl_o}$, we performed a continuation on stationary points of $\mathsf{L}_{\varepsilon=1}(\mathbf{z}, \dot{x}_{\text{avg}})$. That is, rather than keeping $\dot{x}_{\text{avg}}$ constant and varying ε, we kept ε constant and varied $\dot{x}_{\text{avg}}$ (blue line in Fig. 4). When one is interested at optimal gaits over a range of speeds, this process is not only more efficient than individually tracing motions from passive to active, but also reveals something about the structure of the optimal gaits. In particular, we again considered the smallest eigenvalue $\mu_{\min}$ of $\mathbf{H}_M$ while tracing the first order condition towards lower forward speeds $\dot{x}_{\text{avg}}$. As shown in Fig. 4, the blue curve indicates a turning point at $\dot{x}^*_{\text{avg}}$ at which the stationary points become saddle points (dashed line) and are thus no longer optimal gaits.

IV. Discussion & Conclusion

In this paper, we introduced a systematic method for the gait generation of legged robots. It works by linking the passive periodic motions of a legged system's underlying energetically conservative dynamics (w.r.t. eq. (1) and eq. (2))

[1]It took approximately 150 minutes to generate this curve on a laptop with an i5-8265U CPU @1.60GHz and 4GB RAM. The code is available online https://github.com/raffmax/GeneratingFamiliesofOptimallyActuatedGaitsfromaLeggedSystemsEnergeticallyConservativeDynamics

to optimally actuated gaits of a full robot model. Using numerical continuation methods, our approach is based on a model homotopy that continuously connects the full robot model with a non-dissipative version. This homotopy is embedded in a constrained optimization problem (COP). A key insight in this process is the interpretation of the passive gaits as optimal points of the COP. As we showed, this holds for a broad class of energetic cost functions, input parameterizations and operating points.

The most important property of our approach is that it can be started from very basic motions. In our example, this starting point was a simple hopping-in-place motion. Since the passive periodic motions form connected components [4], this starting point can be systematically grown into a range of seeds for our homotopy-based algorithm. Within the algorithm, the seeds are then grown further along stationary curves of the COP that lead to the optimal gaits of the fully dissipative system. As a consequence, optimality is maintained throughout the process. In our example, we only considered a single branch of a passive periodic forward hopping motion to generate these seeds. However, for more complex multi-legged systems, this space of passive gaits is much larger and encompasses a broad range of different gaits with different footfall sequences [5]. We believe that the automated generation of suitable seeds is the biggest advantage of our method in comparison to methods for gait generation which rely on a manually chosen initial guess which must often be based on empirical domain-knowledge.

From a technical point of view, there are currently three main limitations that we continue to work on. First, it would be desirable to have an automated process to generate the non-dissipative model abstraction. The method described in Section III is fairly systematic, but still requires intimate knowledge about the system dynamics. While the scaling of dissipative forces in the continuous dynamics (1) is straight forward, there are potentially better ways to introduce a homotopy in the discrete map (2) without affecting the continuous dynamics and its well-posedness. Secondly, a key assumption in this paper and in [4] is that the contact sequence is fixed. This is needed to guarantee the existence of the derivatives that are necessary for the continuation methods. Being able to relax this assumption would greatly increase the versatility of our approach as it would allow us to connect gaits with different contact sequences, such as walking or running to the same starting point. A third avenue to build up on the model homotopy is to incorporate physical and actuator limitations of the robotic system as well as contact friction models by inequality constraints. For instance, in the motions of our example hopper, the foot actually swings through the ground for the identified families of optimal gaits in ($\varepsilon \in [0, 1]$). To avoid that, inequality constraint must be introduced and reflected in the COP [21].

From a topological perspective, it is an interesting result that the range of optimal forward gaits (the blue line in Fig. 4) does not connect to the passive gaits at low speeds, yet has a turning point at around $\dot{x}^*_{\text{avg}} \approx 0.12\ \sqrt{gl_o}$. Quite obviously, this connectedness and topological structure of the space of optimal gaits is an important feature for our algorithm to work. Understanding how we can provide conditions when a curve $\boldsymbol{\gamma}$ of the COP can be successfully traced from $\varepsilon = 0$ to $\varepsilon = 1$ using the map $\boldsymbol{r}(\mathbf{z}, \varepsilon) = \mathbf{0}$, would hence be a very useful insight. This could potentially be achieved by using other forms of homotopies that build up on functions like $\boldsymbol{r}$, and for which the existence of $\boldsymbol{\gamma}$ can be proven [8], [21]. Such insights would have implications beyond the field of motion generation and robotics, as they would establish fundamental connections between the passive dynamics of simple templates and the gaits that we can observe in nature.

REFERENCES

[1] R. Alexander, "Simple models of walking and jumping," *Human Movement Science*, vol. 11, no. 1, pp. 3–9, 1992.

[2] R. Blickhan, "The spring-mass model for running and hopping," *Journal of Biomechanics*, vol. 22, no. 11-12, pp. 1217–1227, jan 1989.

[3] A. Goswami, *Humanoid robotics : a reference*. Dordrecht: Springer, 2018.

[4] M. Raff, N. Rosa, and C. D. Remy, "Connecting gaits in energetically conservative legged systems," *IEEE Robotics and Automation Letters*, vol. 7, no. 3, pp. 8407–8414, 2022.

[5] Z. Gan, Y. Yesilevskiy, P. Zaytsev, and C. D. Remy, "All common bipedal gaits emerge from a single passive model," *Journal of The Royal Society Interface*, vol. 15, no. 146, p. 20180455, 2018.

[6] N. Rosa and K. M. Lynch, "Extending equilibria to periodic orbits for walkers using continuation methods," in *2014 IEEE/RSJ International Conference on Intelligent Robots and Systems*. IEEE, 2014, pp. 3661–3667.

[7] Z. Gan, Z. Jiao, and C. D. Remy, "On the dynamic similarity between bipeds and quadrupeds: a case study on bounding," *IEEE Robotics and Automation Letters*, vol. 3, no. 4, pp. 3614–3621, 2018.

[8] E. L. Allgower and K. Georg, *Numerical continuation methods: an introduction*. Springer Science & Business Media, 2012, vol. 13.

[9] N. Rosa and K. M. Lynch, "A topological approach to gait generation for biped robots," *IEEE Transactions on Robotics*, pp. 1–20, 2021.

[10] A. Hereid and A. D. Ames, "Frost: Fast robot optimization and simulation toolkit," in *Intelligent Robots and Systems (IROS), 2017 IEEE/RSJ International Conference on*. IEEE, 2017, pp. 719–726.

[11] M. Posa, C. Cantu, and R. Tedrake, "A direct method for trajectory optimization of rigid bodies through contact," *The International Journal of Robotics Research*, vol. 33, no. 1, pp. 69–81, 2014.

[12] M. Fevre, P. M. Wensing, and J. P. Schmiedeler, "Rapid bipedal gait optimization in casadi," in *2020 IEEE/RSJ International Conference on Intelligent Robots and Systems (IROS)*, 2020, pp. 3672–3678.

[13] R. Full and D. Koditschek, "Templates and anchors: neuromechanical hypotheses of legged locomotion on land," *Journal of Experimental Biology*, vol. 202, no. 23, pp. 3325–3332, 12 1999.

[14] B. Brogliato, *Nonsmooth Mechanics: Models, Dynamics and Control*. Springer, 2016.

[15] L. Piegl and W. Tiller, *The NURBS book*. Springer Science & Business Media, 1996.

[16] C. D. Remy, K. Buffinton, and R. Siegwart, "Comparison of cost functions for electrically driven running robots," in *2012 IEEE International Conference on Robotics and Automation*. IEEE, 2012, pp. 2343–2350.

[17] D. G. Luenberger, Y. Ye, *et al.*, *Linear and nonlinear programming*. Springer, 1984, vol. 2.

[18] C. D. Remy, "Optimal exploitation of natural dynamics in legged locomotion," Ph.D. dissertation, ETH Zurich, 2011.

[19] Y. Yesilevskiy, Z. Gan, and C. David Remy, "Energy-optimal hopping in parallel and series elastic one-dimensional monopeds," *Journal of Mechanisms and Robotics*, vol. 10, no. 3, p. 031008, 2018.

[20] A. M. Johnson, S. A. Burden, and D. E. Koditschek, "A hybrid systems model for simple manipulation and self-manipulation systems," *The International Journal of Robotics Research*, vol. 35, no. 11, pp. 1354–1392, 2016.

[21] L. T. Watson, "Theory of globally convergent probability-one homotopies for nonlinear programming," *SIAM Journal on Optimization*, vol. 11, no. 3, pp. 761–780, 2001.